

See discussions, stats, and author profiles for this publication at: <https://www.researchgate.net/publication/231633536>

# Electronic Spectrum of the Gallium Dimer

ARTICLE *in* THE JOURNAL OF PHYSICAL CHEMISTRY A · MARCH 2003

Impact Factor: 2.69 · DOI: 10.1021/jp022089w

---

CITATIONS

21

---

READS

14

## 2 AUTHORS:



Xiaofeng Tan

Johns Hopkins University

25 PUBLICATIONS 183 CITATIONS

SEE PROFILE



Paul J Dagdigian

Johns Hopkins University

323 PUBLICATIONS 6,193 CITATIONS

SEE PROFILE

## Electronic Spectrum of the Gallium Dimer

Xiaofeng Tan and Paul J. Dagdigan\*

Department of Chemistry, The Johns Hopkins University, Baltimore, Maryland 21218-2685

Received: September 18, 2002; In Final Form: January 24, 2003

A study of the electronic spectrum of the gallium dimer in the 33 600–36 800  $\text{cm}^{-1}$  spectral range is presented. The dimer was prepared in a pulsed, free-jet supersonic beam and detected by laser fluorescence excitation and depletion spectroscopy. All observed excited vibronic levels predissociate, and the transitions were detected by observation of Ga 5s  $\rightarrow$  4p atomic emission. Four excited-state progressions were observed, and it was possible to assign the excited-state vibrational quantum numbers on the basis of observed isotope shifts for two of the four progressions. Through comparison of the results with available quantum chemical calculations, these two progressions were assigned as electronic transitions to the  $3^3\Pi_g$  and  $2^1\Pi_g$  states from the ground  $X^3\Pi_u$  state. A Franck–Condon analysis was performed to determine the equilibrium internuclear separation of the  $3^3\Pi_g$  state. An upper limit for the Ga<sub>2</sub> dissociation energy,  $D_e'' < 8891 \text{ cm}^{-1}$ , was derived. This bound is consistent with previous experimental and computational estimates of the dissociation energy.

### 1. Introduction

There continues to be considerable interest in the structure and spectroscopy of metal dimers and small clusters.<sup>1–3</sup> These systems serve as models for developing a detailed understanding of larger clusters and metallic catalysts. Spectroscopic studies using both resonance-enhanced multiphoton ionization and laser fluorescence excitation have provided considerable detailed information on bond lengths, vibrational frequencies, and the character of the electronic states of the dimers of transition and the coinage metals.<sup>4–18</sup> The situation in the middle of the periodic table is considerably less satisfactory. Clouthier and co-workers<sup>19</sup> recently presented the first high-resolution spectroscopic study of the germanium dimer. They reported rotationally resolved spectra, derived structures of the ground and observed excited electronic states, and were able to obtain information on the character of the electronic states. They pointed out the curious fact that the structures and high-resolution electronic spectra of the dimers of a number of elements in the middle of the periodic table (Ga<sub>2</sub>, In<sub>2</sub>, and Tl<sub>2</sub>) remain unknown.

In the course of a search for the electronic spectrum of the Ga–H<sub>2</sub> van der Waals complex, following our studies of the Al–H<sub>2</sub> complex by predissociation spectroscopy,<sup>20–23</sup> we have observed electronic transitions of the gallium dimer in the 33 600–36 800  $\text{cm}^{-1}$  wavenumber range. As mentioned above, the published spectroscopic information available on Ga<sub>2</sub> is quite limited. Ginter et al.<sup>24</sup> reported the observation of emission bands in the wavenumber range 18 200–21 700  $\text{cm}^{-1}$ , but a rotational analysis could not be carried out. Douglas et al.<sup>25</sup> observed several absorption bands of matrix-isolated Ga<sub>2</sub> and suggested a  $X^1\Sigma_g^+$  ground state. In another matrix isolation study, Froben et al.<sup>26</sup> derived a ground-state vibrational frequency of 180  $\text{cm}^{-1}$  by Raman spectroscopy. There have been several mass spectrometric thermochemical studies to determine the Ga<sub>2</sub> bond energy.<sup>27–29</sup> The most recent of these, by Shim et al.<sup>28</sup> and Balducci et al.,<sup>29</sup> yield values of  $D_0$  in good agreement with each other:  $9220 \pm 590 \text{ cm}^{-1}$  and  $9260 \pm 410 \text{ cm}^{-1}$ , respectively. Stowe et al.<sup>30</sup> reported an ESR study of the aluminum and gallium dimer anions and assigned the ground

states of these species as  $4^4\Sigma_g^-$ . Cha et al.<sup>31</sup> have reported the photoelectron spectra of Ga<sub>*n*</sub><sup>–</sup> clusters. These data reveal information about the ground and low-lying excited states of the neutral species.

There have been several quantum chemical calculations on the electronic states of the gallium dimer. Balasubramanian<sup>32</sup> carried out extensive calculations, on both the ground state and a number of excited states, of the neutral and ionic species of the gallium dimer by employing the complete active space MCSCF (CASSCF) method with an effective relativistic core potential, followed by first-order CI (FOCI) and second-order CI (SOC) calculations. A dissociation energy and vibrational frequency of 9680 and 162  $\text{cm}^{-1}$ , respectively, were obtained for the ground electronic state. Das<sup>33</sup> performed CI (MRD-CI) calculations based on relativistic core potentials. In this case, the spin–orbit interaction was included, and potential energy curves for the different low-lying  $\Omega$  levels were computed. These calculations yielded values of 9440 and 162  $\text{cm}^{-1}$  for the ground-state dissociation energy and vibrational frequency, respectively. Ghosh et al.<sup>34</sup> recently reported spectroscopic constants for the low-lying electronic states computed with MRSDCI and MRCPA methods. The calculated vibrational frequency for the ground state were 175 (MRSDCI) and 170  $\text{cm}^{-1}$  (MRCPA), while the calculated ground-state dissociation energy for the ground state is 10400  $\text{cm}^{-1}$  by MRSDCI and 10320  $\text{cm}^{-1}$  by MRCPA. All these theoretical calculations suggest that this is a  $3^3\Pi_u$  ground state, with a very low-lying excited  $3^3\Sigma_g^-$  state. It is assumed that the computed vibrational frequencies apply to the <sup>69</sup>Ga<sub>2</sub> isotopomer.

We report in this paper the observation of vibrational progressions associated with several excited electronic states of the gallium dimer. In all cases, the excited states predissociate, and the transitions were detected by observation of emission from electronically excited Ga 5s atoms produced in the predissociation process. We compare the information obtained on the observed excited states with that available<sup>32,33</sup> from the quantum chemical calculations.

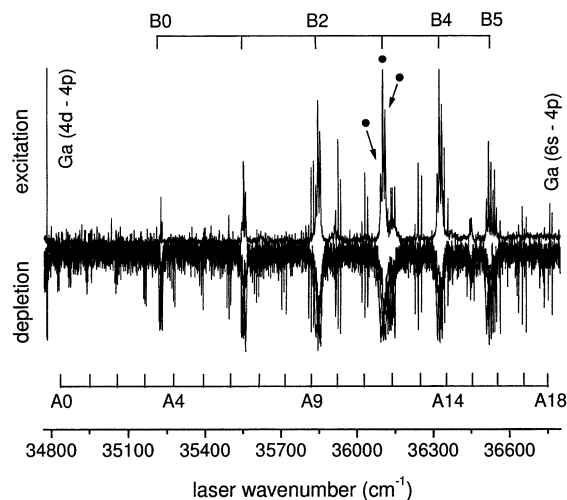


**Figure 1.** Survey laser fluorescence excitation (FE) (top) and fluorescence depletion (FD) (bottom) spectra of  $\text{Ga}_2$  in the wavenumber range 34 800–36 800  $\text{cm}^{-1}$ . Ga atomic  $5s \rightarrow 4p$  emission was monitored while the excitation laser was scanned. The FD spectrum is a composite of three such spectra obtained by setting the probe laser wavenumber to bands centered at 36 111.5, 36 102.7, and 36 093.8  $\text{cm}^{-1}$ . These bands are marked with solid circles in the top panel. The laser power density was 2  $\mu\text{J}/\text{mm}^2$  for the FE and FD probe laser and 20  $\mu\text{J}/\text{mm}^2$  for the FD depletion laser. For the FD spectra, the delay between the depletion and probe lasers was 200 ns. The strongest features in the FD spectra correspond to a depletion of 70%. The bands are assigned to two excited-state vibrational progressions in  $\text{Ga}_2$  and are labeled A0–A18 and B0–B5. The beam seed gas mixture was 20% hydrogen and 80% helium, at a total pressure of 18 atm.

## 2. Experimental Section

The apparatus in which these experiments were carried out has been described in detail previously.<sup>20–22</sup> In brief, the gallium dimer was prepared in a pulsed, free-jet supersonic expansion (0.2 mm diameter orifice) of mixtures of trimethylgallium (TMG, Strem), hydrogen, and helium. Deuterium and argon in various seed gas mixtures were also employed in place of hydrogen. Ga atoms were generated at the nozzle orifice by 193 nm photolysis of TMG. The free-jet beam was interrogated 1.2 cm downstream by fluorescence excitation (FE) and depletion (FD) spectroscopy with the frequency-doubled output of a Nd:YAG laser pumped dye laser, with a bandwidth of 0.1  $\text{cm}^{-1}$ . In the FD experiments, the frequency-doubled signal output of a Continuum Powerlite 8000 Nd:YAG laser pumped Sunlite EX BBO optical parametric oscillator (OPO), with a bandwidth of 0.2  $\text{cm}^{-1}$ , was employed as the depletion laser, while the dye laser was employed as the probe laser.

The transitions were detected by action spectroscopy, in which emission from the excited Ga 5s atoms formed by predissociation was imaged onto a 1/4 m monochromator and detected with a photomultiplier (PMT). The PMT output was directed to a gated integrator and then recorded on a laboratory computer. The laser wavenumber was calibrated with Ga atomic lines and a solid fused-silica Etalon (free spectral range 0.676  $\text{cm}^{-1}$  in the visible).

## 3. Results

**Progressions in the Range 34 800–36 800  $\text{cm}^{-1}$ .** Several progressions were observed over the full scanned wavenumber range of 33 600–36 800  $\text{cm}^{-1}$ . The two progressions occurring above 34 800  $\text{cm}^{-1}$  showed resolvable isotope splittings, and we discuss these progressions first.

The top panel of Figure 1 displays the FE spectrum in the

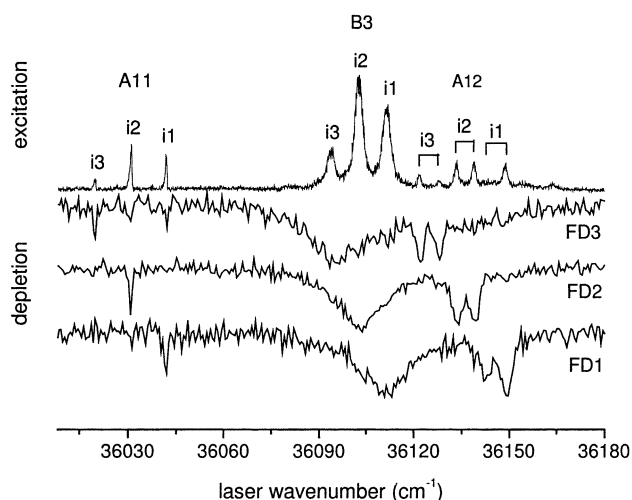


**Figure 2.** Expanded view of the FE (top trace) and FD spectra in the spectral region of bands A11, B3, and A12. Ga atomic  $5s \rightarrow 4p$  emission was monitored while the excitation laser was scanned. The spectra FD1, FD2, and FD3 were recorded by tuning the probe laser to 36 111.5, 36 102.7, and 36 093.8  $\text{cm}^{-1}$ , respectively. The conditions were identical to those noted in the caption of Figure 1.

wavenumber range 34 800–36 800  $\text{cm}^{-1}$ . Two progressions of bands, labeled A and B, are visible in the spectrum. These bands could be observed when emission on either of the fine-structure lines,  $^2S_{1/2} \rightarrow ^2P_{1/2}$  at 403 nm or  $^2S_{1/2} \rightarrow ^2P_{3/2}$  at 417 nm, of the Ga 5s  $\rightarrow$  4p atomic transition was monitored. No other emissions, including resonance fluorescence, were observed when these bands were excited. The relative intensities of the emission lines were 1:1.8, respectively, in good agreement with the known ratio of 1:2.09 of the transition probabilities.<sup>35</sup>

The bands in the prominent progression B in the FE spectrum have larger widths than do the bands in the weaker progression A. In both progressions, each band is composed of three closely spaced features. The spacings between these features vary slightly across a progression. A satisfactory spectral assignment could not be obtained if we assumed that the closely spaced features involve the same molecular carrier. Species considered included  $\text{GaCH}_3$ ,<sup>36</sup> which is likely formed in the photolysis of TMG. The Ga–CH<sub>3</sub> bond energy is, in fact, sufficiently large<sup>37</sup> that Ga 5s atoms cannot be produced upon excitation in this photon energy range.

To identify the molecular carrier(s), FD spectra were recorded, successively tuning the depletion laser to each of the three features (marked with solid circles in Figure 1) of the band near 36 100  $\text{cm}^{-1}$ . The bottom panel of Figure 1 presents a composite of the three FD spectra. The bands of both progressions are displayed quite clearly in the FD spectra. We label the individual bands of the progression with small wavenumber spacings and narrow bandwidths as A0–A18, while the bands in the progression with large spacings and broad bandwidths are labeled B0–B5. Many of the bands in progression A do not appear in the FE spectrum, particularly those at lower transition wavenumbers.

A detailed view of the portion of the FE and FD spectra which includes bands A11, B3, and A12 is displayed in Figure 2. The three FD spectra obtained with the depletion laser tuned to each of the three features of the band near 36 100  $\text{cm}^{-1}$  are separately plotted. The individual features associated with each band are labeled i1, i2, and i3. It can be seen that only one of the three features (low-frequency, middle, or high-frequency) associated with each band in both progressions appears in a given FD spectrum (FD1, FD2, or FD3). This is true also for the

superimposed FD spectra plotted in Figure 1. This implies that there are three molecular carriers for the spectra plotted in Figures 1 and 2. We note that there are two naturally occurring gallium isotopes, namely  $^{69}\text{Ga}$  and  $^{71}\text{Ga}$ , with abundances of 60.4 and 39.6%, respectively.<sup>38</sup> A molecule containing two Ga atoms, for example  $\text{Ga}_2$ , would have the following isotopic abundances: 36.5% for  $^{69}\text{Ga}_2$ , 47.8% for  $^{69}\text{Ga}^{71}\text{Ga}$ , and 15.7% for  $^{71}\text{Ga}_2$ . These abundances agree very well with the relative intensities of features i1, i2, and i3, respectively, in the FE spectra displayed in Figures 1 and 2. Thus, we conclude that the molecular carrier contains two Ga atoms.

The observation of  $\text{Ga } 5s \rightarrow 4p$  emission upon laser excitation in the spectral region displayed in Figure 1, as a result of formation of  $\text{Ga } 5s$  fragments from predissociation of the excited level, is consistent with the energetics of the process  $\text{Ga}_2^* \rightarrow \text{Ga}(4p) + \text{Ga}(5s)$ , based on the above quoted experimental and computed bond energies of the gallium dimer. The spectral features shown in Figure 1 disappeared if TMG were removed from the seed gas mixture or the photolysis laser was turned off and are unchanged if hydrogen was replaced with deuterium. With argon/helium/TMG seed gas mixtures, additional features were observed; this is suggestive of a higher vibrational temperature in these cases. Broad, unresolved features were observed with helium/TMG seed gas mixtures, indicative of inefficient cooling in this case. The above observations are consistent with the assignment of the molecular carrier of the observed bands as  $\text{Ga}_2$ , which is formed in termolecular collisions in the free-jet expansion. In previous work,<sup>23,39</sup> we have also observed  $\text{Al}_2$  and  $\text{B}_2$  in supersonic free-jet expansions with photolyzed trimethylaluminum and diborane, respectively.

The assignment of the features i1, i2, and i3 to the  $^{69}\text{Ga}_2$ ,  $^{69}\text{Ga}^{71}\text{Ga}$ , and  $^{71}\text{Ga}_2$  isotopomers, respectively, is consistent with the assignment of the observed bands as excited-state vibrational progressions. The isotopomer with the largest reduced mass ( $^{71}\text{Ga}_2$ ) would be expected to have the smallest vibrational energies and hence have the lowest-frequency transition within a given band. The assignment of features i3 to  $^{71}\text{Ga}_2$  is in concert with this expectation and the calculated abundances of the isotopomers. In further support of our assignment of the molecular carrier as  $\text{Ga}_2$ , we note that these Ga isotope splittings are larger than would be consistent with a molecular carrier involving two Ga atoms and the light atoms C and possibly H. We also note that the presence of both progressions, A and B, in the FD spectra means that these progressions involve transitions from the same lower vibronic state, presumably the  $v'' = 0$  vibrational level of the  $X^3\Pi_u$  electronic state.

The individual bands in features B0–B5 are broad and are found to be well-fitted with Lorentzian profiles. Table 1 presents the measured transition wavenumbers  $T_v$  of the band centers and fitted full widths at half-maximum (fwhm) of the Lorentzian widths  $\Gamma$  for the observed bands of all isotopomers in progression B. The widths and transition wavenumbers were derived from nonlinear least-squares fits to the profiles of individual bands. The bands in progression A are significantly narrower than those in B. Nonlinear least-squares fits of the profiles of the former were also performed. The derived transition wavenumbers of the band centers and Lorentzian widths for bands of progression A are listed in Table 2. The widths of the bands were derived from analysis of the bands in the FE spectra, for reasons discussed below. These quoted widths are large enough that the rotational structure of the bands would be totally obscured.

We see in Figure 2 that band A12 is split into two features for each isotopomer. This implies that the upper vibronic level

**TABLE 1: Transition Wavenumbers and Lorentzian Widths for Bands in Progression B of the Gallium Dimer**

band <sup>a</sup>	$v'$ <sup>b</sup>	$T_v$ <sup>c</sup> (cm <sup>-1</sup> )	$\Gamma$ (cm <sup>-1</sup> )
B0	2	35 230.6/35 231.4 <sup>d</sup>	$1.0 \pm 0.1/1.5 \pm 0.1^d$
		35 225.2/35 226.0 <sup>d</sup>	$1.0 \pm 0.2/1.3 \pm 0.2^d$
		35 219.6/35 221.3 <sup>d</sup>	$1.6 \pm 0.7/1.6 \pm 0.7^d$
B1	3	35 558.9	$3.2 \pm 0.3$
		35 551.3	$2.8 \pm 0.2$
		35 544.3	$2.0 \pm 0.5$
B2	4	35 853.6	$3.2 \pm 0.3$
		35 845.3	$3.3 \pm 0.3$
		35 836.9	$2.9 \pm 0.7$
B3	5	36 111.5	$4.1 \pm 0.4$
		36 102.7	$3.5 \pm 0.3$
		36 093.8	$3.2 \pm 1.2$
B4	6	36 333.7	$3.1 \pm 0.2$
		36 324.7	$3.1 \pm 0.2$
		36 315.5	$4.0 \pm 0.6$
B5	7	36 528.1	$3.0 \pm 0.3$
		36 519.6	$2.7 \pm 0.1$
		36 510.8	$3.1 \pm 0.2$

<sup>a</sup> The entries for  $T_v$  and  $\Gamma$  for each band are given for the  $^{69}\text{Ga}_2$ ,  $^{69}\text{Ga}^{71}\text{Ga}$ , and  $^{71}\text{Ga}_2$  isotopomers in the order of top to bottom. <sup>b</sup> The excited-state vibrational quantum number. See text for discussion of the assignment. <sup>c</sup> Estimated absolute uncertainties  $0.2 \text{ cm}^{-1}$ . <sup>d</sup> This band is perturbed by a nearby dark level, and each feature splits into two peaks, whose transition wavenumbers and Lorentzian widths are reported.

of this band is perturbed by a nearby vibrational level of another, “dark” electronic state. The relative intensities of the extra features in the FE spectrum reflect the relative weights of the “bright” level in the mixed levels, which appears not to be the same for the different isotopomers. The widths of the main and extra features in band A in the FE spectrum are somewhat greater than for other bands in progression A; e.g. see band A11 displayed in Figure 2. This suggests that the perturbing state is more strongly coupled to the dissociation continuum than the bright electronic state. Besides band A12, bands A16 and B0 were also found to be perturbed by nearby dark levels.

The widths of the bands are seen in Figure 2 to be different in the FE and FD spectra. The widths reported in Tables 1 and 2 refer to bands observed in the FE spectrum. The larger widths in the FD spectra reflect power broadening since a higher laser energy was employed for the depletion laser in recording the FD spectra than for the excitation laser for the FE spectra.

It was not possible to assign the excited-state vibrational quantum numbers  $v'$  by a simple examination of the individual spectra of the  $\text{Ga}_2$  isotopomers since it was not clear that the band with the lowest transition wavenumber in either progression has  $v' = 0$ . The vibrational assignments were carried out in the following manner. For a given progression, the transition wavenumber for a  $(v', 0)$  band of a given  $\text{Ga}_2$  isotopomer (i) can be written as<sup>40</sup>

$$T_v^{(i)} = T_{00} + \rho_i \omega_e' v' - \rho_i^2 \omega_e x_e' v'(v' + 1) + \rho_i^3 \omega_e y_e' v'[(v')^2 + (3/2)v' + (3/4)] + [\text{ZPE}^{(i)} - \text{ZPE}'] - [\text{ZPE}''^{(i)} - \text{ZPE}''] \quad (1)$$

where  $T_{00}$  is the transition wavenumber of the origin and band and  $\omega_e'$ ,  $\omega_e x_e'$ , and  $\omega_e y_e'$  are the upper-state vibrational constants for the reference isotopomer (taken to be  $^{69}\text{Ga}_2$ ). The terms denoted  $\text{ZPE}^{(i)}$  and  $\text{ZPE}$  are zero-point energies of appropriate electronic states (denoted by the single and double primes) of the isotopomer under consideration and the reference isotopomer. The factor  $\rho_i$  is unity for the reference isotopomer and equals the reduced mass ratio  $[\mu(^{69}\text{Ga}_2)/\mu(^i\text{Ga}_2)]^{1/2}$  for the  $i$ th



**TABLE 2: Transition Wavenumbers and Lorentzian Widths for Bands in Progression A of the Gallium Dimer**

band <sup>a</sup>	$v'$ <sup>b</sup>	$T_v^c$ (cm <sup>-1</sup> )	$\Gamma^d$ (cm <sup>-1</sup> )
A0	4	34 829.0	
		34 826.0	
		34 823.0	
A1	5	34 942.8	
		34 939.2	
		34 935.6	
A2	6	35 056.5	
		35 051.7	
		35 047.4	
A3	7	35 168.9	
		35 163.4	
		35 158.0	
A4	8	35 280.5	
		35 274.5	
		35 268.4	
A5	9	35 391.4	
		35 384.8	
		35 377.6	
A6	10	35 501.6	
		35 494.4	
		35 486.6	
A7	11	35 611.1	
		35 603.3	
		35 594.9	
A8	12	35 719.9	
		35 710.9	
		35 701.9	
A9	13	35 827.8	0.8 ± 0.2
		35 818.2	0.7 ± 0.2
		35 808.4	1.1 ± 0.6
A10	14	35 935.1	1.0 ± 0.4
		35 924.7	1.1 ± 0.2
		35 914.3	1.1 ± 0.3
A11	15	36 041.7	0.6 ± 0.2
		36 030.7	0.6 ± 0.2
		36 019.5	1.1 ± 0.6
A12	16	36 143.3/36 148.9 <sup>e</sup>	$f/1.9 \pm 0.3^e$
		36 133.4/36 138.9 <sup>e</sup>	$1.6 \pm 0.4/2.0 \pm 0.3^e$
		36 121.9/36 128.1 <sup>e</sup>	$2.2 \pm 0.6/1.9 \pm 0.9^e$
A13	17	36 252.9	1.1 ± 0.6
		36 240.5	0.9 ± 0.3
		36 228.1	1.0 ± 0.5
A14	18	36 357.1 ± 0.04 <sup>g</sup>	0.9 ± 0.3 <sup>g</sup>
		36 344.0 ± 0.04 <sup>g</sup>	1.0 ± 0.5 <sup>g</sup>
		36 460.9	
A15	19	36 447.2	
		36 433.4	
		36 543.1/36 564.0 <sup>e</sup>	$0.7 \pm 0.2/0.7 \pm 0.2^e$
A16	20	36 536.6/36 549.7 <sup>e</sup>	$0.4 \pm 0.2/2.3 \pm 0.7^e$
		36 529.4/36 535.4 <sup>e</sup>	$f$
		36 666.4	
A17	21	36 651.6	
		36 636.4	
		36 768.2	
A18	22	36 752.7	
		36 736.7	

<sup>a</sup> The entries for  $T_v$  and  $\Gamma$  for each band are given for the <sup>69</sup>Ga<sub>2</sub>, <sup>69</sup>Ga<sup>71</sup>Ga, and <sup>71</sup>Ga<sub>2</sub> isotopomers in the order of top to bottom. <sup>b</sup> The excited-state vibrational quantum number. See text for discussion of the assignment. <sup>c</sup> Estimated absolute uncertainties 0.2 cm<sup>-1</sup>. <sup>d</sup> Lorentzian widths reported only for bands observed in the FE spectrum. See text. <sup>e</sup> This band is perturbed by a nearby dark level, and each feature splits into two peaks, whose transition wavenumbers and Lorentzian widths are reported. <sup>f</sup> Lorentzian width not reported since this band was observed only in FD spectra. <sup>g</sup> Reported values for this band are for <sup>69</sup>Ga<sub>2</sub> and <sup>69</sup>Ga<sup>71</sup>Ga only, since the transition for <sup>71</sup>Ga<sub>2</sub> is obscured by band B4 of progression B.

isotopomer. The excited-state zero-point energy ZPE' can, of course, be written in terms of the excited-state vibrational constants. We can thus rewrite eq 1 to read

$$T_v^{(i)} = T_{00} + \omega_e'[\rho_i v' + (1/2)(\rho_i - 1)] - \omega_e x_e'[\rho_i^2 v'(v' + 1) - (1/4)(\rho_i^2 - 1)] + \omega_e y_e'[\rho_i^3 v'((v')^2 + (3/2)v' + (3/4)) - (1/8)(\rho_i^3 - 1)] - [ZPE''^{(i)} - ZPE''] \quad (2)$$

Linear least-squares fits of eq 2 to the transition wavenumbers for the bands of the three isotopomers of a given progression (A or B) were carried out with various  $v'$  assignments. Using the observed<sup>26</sup> ground-state vibrational frequency of 180 cm<sup>-1</sup>, estimates of  $[ZPE''^{(i)} - ZPE'']$  equaling -0.64 and -1.28 cm<sup>-1</sup> were obtained for <sup>69</sup>Ga<sup>71</sup>Ga, and <sup>71</sup>Ga<sub>2</sub>, respectively. Bands A12 and A16 were excluded from the fits of progression A because of the above-noted perturbations of these bands. Because of the limited data set for progression B, the mean transition wavenumbers of the main and extra features of band B0 were included.

From these fits, we conclude that the first observed band in progression B (B0) has  $v' = 2$ . The assigned  $v'$  quantum numbers of all the bands in this progression are given in Table 1. This assignment seems secure since the  $\chi^2$  of the fit increased by a factor of 5 if the  $v'$  quantum numbers were changed by  $\pm 1$ . The following spectroscopic parameters for <sup>69</sup>Ga<sub>2</sub> were obtained in the fit:  $T_{00} = 34\,457.3 \pm 1.0$ ,  $\omega_e' = 447.421 \pm 0.010$ ,  $\omega_e x_e' = 20.888 \pm 0.218$ ,  $\omega_e y_e' = 0.2570 \pm 0.0146$ . For progression A, we determine that  $v' = 4$  for band A0. In this case, the  $\chi^2$  of the fit increased by more than an order of magnitude if the  $v'$  quantum numbers were changed by  $\pm 1$ . The fitted  $\omega_e y_e'$  parameter was not statistically significant and was dropped from the final fits. The following spectroscopic parameters for progression A of <sup>69</sup>Ga<sub>2</sub> were determined:  $T_{00} = 34\,366.58 \pm 0.16$ ,  $\omega_e' = 117.488 \pm 0.028$ ,  $\omega_e x_e' = 0.362\,69 \pm 0.0104$ .

No information is available from the experimental measurements on the rotational constants, and hence the length scale of potential energy curves supporting these two progressions. Instead, we have carried out a Franck–Condon analysis of the intensities of the bands in a given progression and compared the computed band strengths with the relative intensities in the FE spectrum. This presumes that the observed Ga 5s → 4p emission intensity accurately reflects the absorption strengths for transitions to the various excited vibrational levels. From a comparison of the relative intensities of the bands in the FE and FD spectra (see Figure 1), this seems a reasonable assumption for progression B. We take the intensities from the FE spectrum since the intensities are saturated in the FD spectrum.

By contrast, the bands in progression A are largely absent in the FE spectrum for transition wavenumbers below that of A9, while the bands at lower wavenumbers still appear strongly in the FD spectrum. This suggests that the lower  $v'$  levels decay nonradiatively, through formation of ground-state Ga 4p atoms, rather than formation of Ga(4p) + Ga(5s) fragments. Thus, the intensities in the FE spectrum cannot be equated with the absorption strengths of the bands, and a Franck–Condon analysis was not carried out for progression A.

An RKR procedure<sup>41</sup> was used to generate a potential energy curve of the upper state of progression B. A vibrational energy expression  $G(v')$  using the derived vibrational constants given above was employed. It should be noted that  $G(v')$  determines the difference between the inner and outer turning points as a function of energy.<sup>41</sup> Determination of the inner and outer turning points separately requires an expression for the rotational constant as a function of  $v'$ , and a linear expression  $B(v') = B_e' - \alpha_e'(v' + 1/2)$  was assumed here. It is well-known that  $B_e'$  is

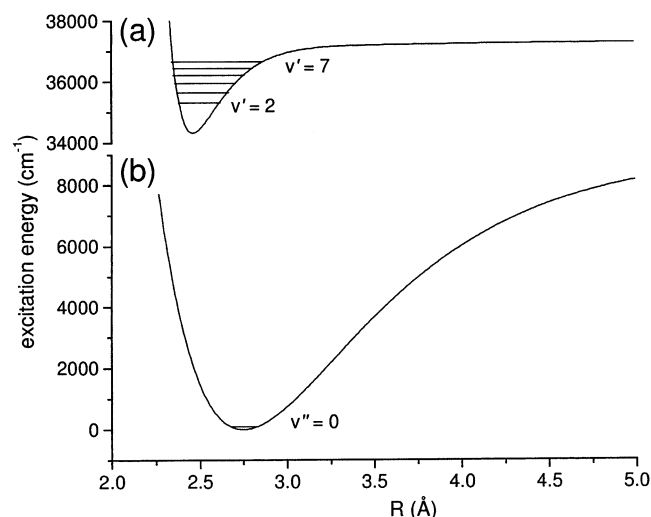


**Figure 3.** Lower panel: Morse potential energy function describing the ground  $X^3\Pi_u$  electronic state of  $\text{Ga}_2$ . Upper panel: potential energy curve describing the excited state (assigned as the  $3^3\Pi_g$  state) of progression B, derived by a Franck–Condon analysis, as described in the text.

determined by the equilibrium internuclear separation.<sup>40</sup> In the RKR procedure,  $\alpha_e'$  affects the slopes of the inner and outer limbs of the potential. For a given value of  $B_e'$ , there is a relatively narrow range of  $\alpha_e'$  values that yield physically reasonable potentials. The potential energy curve was extrapolated beyond the energy range covered by the observed vibrational levels ( $v' > 7$ ) by inverse power law functions, and the dissociation asymptote was taken to be that implied by an extrapolation of the fitted vibrational constants.

A Morse function,<sup>40</sup> with parameters  $D_e'' = 8980 \text{ cm}^{-1}$ ,  $R_e'' = 2.748 \text{ \AA}$ , and  $\beta = 1.357 \text{ \AA}^{-1}$ , was assumed for the ground  $X^3\Pi_u$  electronic state of  $^{69}\text{Ga}_2$ . The dissociation energy comes from the present study, and its determination is described below. The equilibrium internuclear separation was taken from the computational study by Das,<sup>33</sup> and the value of  $\beta$  was chosen so that the computed vibrational frequency reproduced the experimental<sup>26</sup> value of  $180 \text{ cm}^{-1}$ . This potential energy curve is plotted in Figure 3b.

For a given assumed excited-state potential defined by the choices of  $B_e'$  and  $\alpha_e'$  and the fitted vibrational constants, excited-state vibrational wave functions and Franck–Condon factors for the transition from the ground  $v'' = 0$  vibronic level were computed. The rotational parameters (principally  $B_e'$ ) were adjusted until a reasonable agreement of the computed Franck–Condon factors with the experimental FE band intensities in progression B was obtained. Figure 4 presents a comparison of the experimental and computed band intensities for the  $^{69}\text{Ga}_2$  isotopomer. A similar agreement of intensities was found for the other isotopomers. The rotational parameters defining the excited-state potential energy curve are  $B_e' = 0.0808 \text{ cm}^{-1}$  and  $\alpha_e' = 0.0014 \text{ cm}^{-1}$ . The  $B_e'$  value corresponds to an equilibrium internuclear separation  $R_e'$  of  $2.46 \text{ \AA}$ . The uncertainties in  $R_e'$  and  $\alpha_e'$  are estimated to be  $\pm 0.013 \text{ \AA}$  and  $\pm 0.0005 \text{ cm}^{-1}$ , respectively.

Figure 3a presents a plot of the derived excited-state potential energy curve. It can be seen that the equilibrium internuclear separation of this state is significantly smaller than for the  $X^3\Pi_u$  electronic state and the excited-state potential curve considerably narrower than that of the ground state. We defer until the Discussion a comparison of these experimental results with the results from quantum chemical calculations.<sup>32,33</sup>

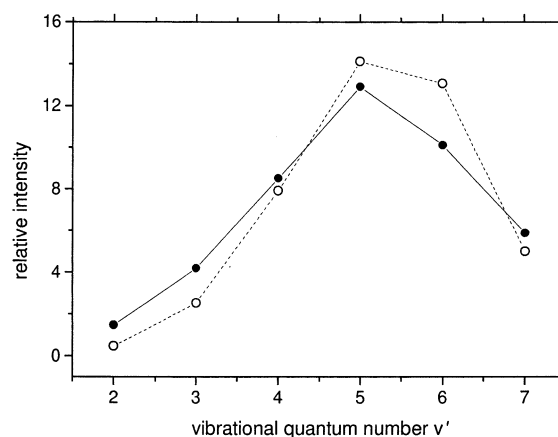


**Figure 4.** Relative intensities of  $^{69}\text{Ga}_2$  bands in progression B. The solid circles are the experimentally observed relative intensities in the FE spectrum, while the open circles are the computed Franck–Condon factors based on the potential energy curves displayed in Figure 3.

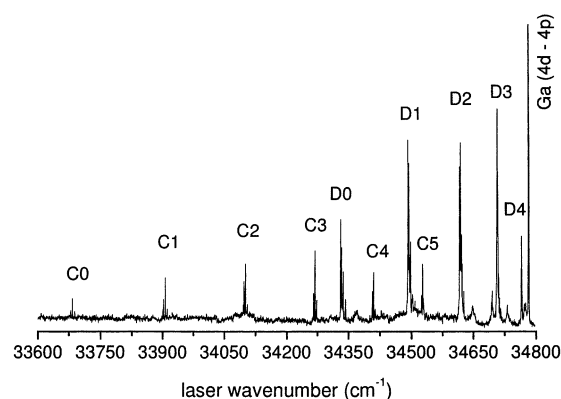


**Figure 5.** Survey laser fluorescence excitation (FE) spectrum of  $\text{Ga}_2$  in the range  $33\,600\text{--}34\,800 \text{ cm}^{-1}$ . Ga atomic  $5s \rightarrow 4p$  emission was monitored while the excitation laser (power density  $2 \mu\text{J}/\text{mm}^2$ ) was scanned. The bands are assigned to two excited-state vibrational progressions in  $\text{Ga}_2$  and are labeled C0–C5 and D0–D4. The beam seed gas mixture was 20% hydrogen and 80% helium, at a total pressure of 18 atm.

**Progressions in the Region  $33\,600\text{--}34\,800 \text{ cm}^{-1}$ .** To the red of the two progressions A and B discussed in the previous subsection, two additional progressions of bands were also observed in FE spectral scans below  $34\,800 \text{ cm}^{-1}$ . These bands were also detected by action spectroscopy, in which Ga  $5s \rightarrow 4p$  atomic emission was monitored while the excitation wavelength was scanned. Again, these bands were only observed with TMG in the seed gas mixture and with the photolysis laser operating.

Figure 5 presents a survey scan of the FE spectrum in this wavenumber range. The two observed progressions are labeled C0–C5 and D0–D4. The upper trace in Figure 6 presents an expanded FE scan of bands C4 and D0 in the two progressions. It can be seen that, unlike the bands in progressions A and B, some structure in the bands, different for the two progressions, is evident. The other bands of progression C showed structure similar to that displayed for band C4, and likewise other bands in progression D were qualitatively similar to band D0.

We verified by FD spectroscopy that the molecular carrier of these bands was the same as for progressions A and B. The probe transitions in band B3, marked with solid circles in Figure 1, were employed in FD scans for each of the isotopomers. The lower three traces in Figure 6 present these FD spectra for bands C4 and D0. The depletion signal was relatively weak for both

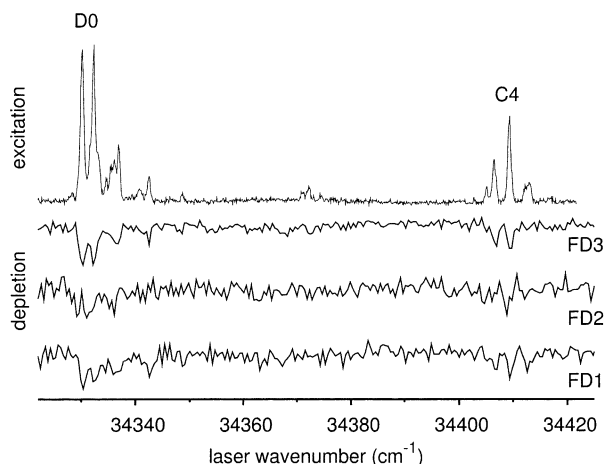


**Figure 6.** Expanded view of the FE (top trace) and FD spectra in the spectral region of bands C4 and D0. The spectra FD1, FD2, and FD3 were recorded by tuning the probe laser to 36 111.5, 36 102.7, and 36 093.8  $\text{cm}^{-1}$ , respectively, and correspond to detection of the  $^{69}\text{Ga}_2$ ,  $^{69}\text{Ga}^{71}\text{Ga}$ , and  $^{71}\text{Ga}_2$  isotopomers. The conditions under which these spectra were recorded were identical as those for the spectrum displayed in Figure 5.

progressions C and D, and the signal-to-noise ratio of the FD spectra was correspondingly poor. Other bands, in particular the higher bands of progression D were significantly broader than in the FE spectra, presumably because of power broadening at the depletion laser energies required for observation of the FD signals. We see from comparison of the FD and FE signals in Figure 6 that the features within a given band in the FE scans are not due to the different isotopomers of  $\text{Ga}_2$ .

As illustrated in Figure 6 for bands C4 and D0, comparison of the FD spectra for the different isotopomers suggests that the isotope shifts of the bands are small. In view of the poor signal-to-noise ratio of the FD spectra and the unassigned structure in each band, no attempt was made to assign excited-state vibrational quantum numbers in these progressions.

We scanned to the red of band C0 to search for lower-wavenumber  $\text{Ga}_2$  transitions detectable by action spectroscopy, wherein emission from excited Ga 5s fragments was monitored. No such transitions were found. This can be used to set an upper bound on the  $\text{Ga}_2$  dissociation energy. This upper limit for  $D_0''$  can be computed from the transition wavenumber  $T_{C0}$  of the red-most band (C0) observed in the action spectrum through the following equation:

$$D_0'' \leq T_{C0} - \nu_{\text{at.}} \quad (3)$$

Here,  $\nu_{\text{at.}}$  is the energy of the Ga 5s  $^2\text{S}$  state relative to the ground Ga  $^2\text{P}_{1/2}$  state.<sup>35</sup> If we take for  $T_{C0}$  the transition wavenumber of the red-most feature in band C0, then we obtain  $D_0'' \leq 8891 \text{ cm}^{-1}$ . This upper bound is within the error limits of the dissociation energies of  $\text{Ga}_2$  determined by thermochemical mass spectrometry.<sup>28,29</sup> The value  $D_0'' = 9440 \text{ cm}^{-1}$  reported by Das<sup>33</sup> is the spin-free dissociation energy. Correcting for the known<sup>35</sup> Ga atomic spin-orbit splitting and the calculated<sup>33</sup> fine-structure energies of  $\text{Ga}(\text{X}^3\Pi_u)$ , we obtain a value of  $8565 \text{ cm}^{-1}$  for the energy to dissociate the ground  $\Omega = 0_u^-$  fine-structure manifold to  $\text{Ga}(4p \ ^2\text{P}_{1/2}) + \text{Ga}(4p \ ^2\text{P}_{1/2})$ . This value is consistent with our estimated upper bound.

We present in Table 3 the transition wavenumbers  $T_v$  and the derived Lorentzian widths  $\Gamma$  for the strongest features observed in each of the bands in progression C. An arbitrary vibrational numbering is given. It can be seen that the widths associated with these transitions are smaller than those of the

**TABLE 3: Transition Wavenumbers and Lorentzian Widths for Bands in Progression C of the Gallium Dimer**

band	$\nu'$ <sup>a</sup>	$T_v^b$ ( $\text{cm}^{-1}$ )	$\Gamma^c$ ( $\text{cm}^{-1}$ )
C0	x	33 683.2	0.3
C1	$x + 1$	33 906.0	0.3
C2	$x + 2$	34 100.7	0.3
C3	$x + 3$	34 268.2	0.5
C4	$x + 4$	34 409.5	0.5
C5	$x + 5$	34 526.5	0.5

<sup>a</sup> An arbitrary excited-state vibrational quantum numbering given since these quantum numbers could not be assigned. <sup>b</sup> Transition wavenumber of the strongest feature within each band; estimated absolute uncertainties  $0.2 \text{ cm}^{-1}$ . <sup>c</sup> Estimated uncertainties  $0.1 \text{ cm}^{-1}$ .

**TABLE 4: Transition Wavenumbers and Lorentzian Widths for Bands in Progression D of the Gallium Dimer**

band	$\nu'$ <sup>a</sup>	$T_v^b$ ( $\text{cm}^{-1}$ )	$\Gamma^c$ ( $\text{cm}^{-1}$ )
D0	y	34 330.3	0.7
D1	$y + 1$	34 491.2	0.9
D2	$y + 2$	34 616.1	0.7
D3	$y + 3$	34 706.3	1.2
D4	$y + 4$	34 764.1	1.2

<sup>a</sup> An arbitrary excited-state vibrational quantum numbering given since these quantum numbers could not be assigned. <sup>b</sup> Transition wavenumber of the red-most feature within each band; estimated absolute uncertainties  $0.2 \text{ cm}^{-1}$ . <sup>c</sup> Estimated uncertainties  $0.1 \text{ cm}^{-1}$ .

bands in progressions A and B. Assuming that the arbitrary vibrational quantum number  $x = 0$ , we obtain the following the excited-state vibrational constants:  $\omega_e' = 247.98 \pm 0.20$  and  $\omega_e x_e' = 13.261 \pm 0.033$ . It should be noted that with these constants, band C4 of the  $^{69}\text{Ga}^{71}\text{Ga}$  isotopomer is predicted to be shifted to the red of the corresponding band of  $^{69}\text{Ga}_2$  by  $3.6 \text{ cm}^{-1}$ , with a similar displacement between the bands of  $^{71}\text{Ga}_2$  and  $^{69}\text{Ga}^{71}\text{Ga}$  [compare with the FD spectra in Figure 6].

Table 4 presents the transition wavenumbers and derived Lorentzian widths of the red-most features within each of the bands in progression D. The widths of these bands are somewhat larger than for the bands in progression C. As with progression C, an arbitrary vibrational numbering has been given to the bands. Assuming that  $y = 0$ , we derive the following excited-state vibrational constants:  $\omega_e' = 194.31 \pm 0.27$  and  $\omega_e x_e' = 17.206 \pm 0.053$ . With these constants, only a small isotope shift is predicted for band D0 [ $\Delta T = -0.1 \text{ cm}^{-1}$  for  $^{69}\text{Ga}^{71}\text{Ga}$  relative to  $^{69}\text{Ga}_2$ ; compare with the FD spectra in Figure 6].

#### 4. Discussion

The predictions from the most recent ab initio calculation by Das<sup>33</sup> on the bound electronic states of  $\text{Ga}_2$  are summarized in Table 5. With minor exceptions, the calculations by Balasubramanian<sup>32</sup> agree with these results. Table 5 presents calculated excitation energies  $T_e$ , equilibrium internuclear separations  $R_e$ , and harmonic vibrational frequencies  $\omega_e$  for the ground  $\text{X}^3\Pi_u$  state and excited states with  $T_e > 20\,000 \text{ cm}^{-1}$ . Bound electronic states with lower excitation energies all correlate with the ground-state asymptote  $\text{Ga}(4p) + \text{Ga}(4p)$ .

Through fluorescence depletion spectroscopy, we have verified that all the observed progressions involve the same lower level of  $\text{Ga}_2$ . This is undoubtedly the  $\nu'' = 0$  level of the ground  $\text{X}^3\Pi_u$  state. We would like to correlate the upper states of the observed progressions with the calculated electronic states, shown in Table 5. We also indicate in Table 5 whether the excited state can be reached by a spin-allowed ( $\Delta S = 0$ ) or spin-forbidden ( $\Delta S \neq 0$ ) electric-dipole transition from the ground  $\text{X}^3\Pi_u$  state.



**TABLE 5: Calculated Properties of the Electronic States of Ga<sub>2</sub><sup>a</sup>**

state	$T_e$ (cm <sup>-1</sup> )	$R_e$ (Å)	$\omega_e$ (cm <sup>-1</sup> )	ED <sup>b</sup>
X <sup>3</sup> Π <sub>u</sub>	0	2.75	162	
3 <sup>3</sup> Σ <sub>u</sub>	20 708	2.68	167	
1 <sup>1</sup> Δ <sub>u</sub>	27 262	2.74	164	
2 <sup>3</sup> Π <sub>g</sub>	28 200	3.06	86	SA
2 <sup>3</sup> Δ <sub>u</sub>	29 585	2.39	274	
1 <sup>1</sup> Σ <sub>u</sub> <sup>+</sup>	32 521	2.79	157	
3 <sup>3</sup> Π <sub>g</sub>	34 189	2.52	313	SA
2 <sup>1</sup> Π <sub>g</sub>	35 089	3.13	63	SF
3 <sup>3</sup> Σ <sub>g</sub>	39 216	2.72	187	SA
3 <sup>1</sup> Π <sub>g</sub>	41 096	2.45	320	SF
4 <sup>3</sup> Π <sub>g</sub>	42 904	2.85	128	SA
3 <sup>1</sup> Δ <sub>g</sub>	42 929	2.94	97	SA
4 <sup>1</sup> Π <sub>g</sub>	48 002	2.62	197	SF

<sup>a</sup> Ref 33. Spin-orbit interaction not included in the calculations. States listed include the ground state and calculated bound states with  $T_e > 20\,000$  cm<sup>-1</sup>. <sup>b</sup> An entry in this column indicates that the transition to this state from the X<sup>3</sup>Π<sub>u</sub> state is electric-dipole allowed. SA denotes a spin-allowed transition, while SF indicates that the transition is nominally spin-forbidden.

We assign the 3<sup>3</sup>Π<sub>g</sub> state as the upper electronic state of progression B. A radiative transition from the X<sup>3</sup>Π<sub>u</sub> state is fully allowed to this state. The agreement of our derived (34 457 cm<sup>-1</sup>) and the computed<sup>33</sup> (34 189 cm<sup>-1</sup>) excitation energy  $T_e$  is quite good. The 3<sup>3</sup>Π<sub>g</sub> state is computed to have a large vibrational frequency and small equilibrium internuclear separation, similar to that determined for the upper state of progression for these quantities by the vibrational fit and Franck-Condon analysis, respectively. From the Franck-Condon analysis, we estimate  $R_e = 2.46$  Å, which is in reasonable agreement with the computed<sup>33</sup> value of 2.52 Å.

The agreement of the vibrational frequencies [ $\omega_e = 447$  (expt), 313 (calc<sup>33</sup>) cm<sup>-1</sup>] is only qualitative. However, in the isovalent Al<sub>2</sub> molecule, Yarkony and co-workers<sup>42</sup> showed that there are strong nonadiabatic couplings of the 1,2,3<sup>3</sup>Π<sub>g</sub> states which strongly affect the energies and also the decay properties of the vibronic levels. A similar nonadiabatic mixing could be occurring here in Ga<sub>2</sub>. Balasubramanian<sup>32</sup> predicts that the 3<sup>3</sup>Π<sub>g</sub> state dissociates to the Ga(4p) + Ga(5p) asymptote, which lies 10 330 cm<sup>-1</sup> above Ga(4p) + Ga(5s). Extrapolation with the presently derived vibrational constants predicts a much lower dissociation asymptote (see Figure 3a). Excited-state mixing may invalidate such an extrapolation.

Predissociation of the 3<sup>3</sup>Π<sub>g</sub> state can occur through coupling to the 2<sup>3</sup>Π<sub>u</sub> state (not listed in Table 5), which correlates with the Ga(4p) + Ga(5s) asymptote. This state is predicted<sup>32</sup> to have a shallow attractive well and to cross the outer limb of the 3<sup>3</sup>Π<sub>g</sub> state. Coupling of these states would provide a mechanism for formation of emitting Ga 5s atoms upon laser excitation of the 3<sup>3</sup>Π<sub>g</sub> state.

A reasonable assignment for the upper state of progression A is the 2<sup>1</sup>Π<sub>g</sub> state. While a radiative transition to this state from the ground X<sup>3</sup>Π<sub>u</sub> state is spin-forbidden, we might expect that singlet-triplet mixing would enable this transition. From the relative integrated intensities of the bands in progressions A and B, we conclude that the strength of the transition to the 2<sup>1</sup>Π<sub>g</sub> state is less than that to the 3<sup>3</sup>Π<sub>g</sub> state, which is spin-allowed. The 2<sup>1</sup>Π<sub>g</sub> state does have a computed<sup>33</sup> excitation energy  $T_e$  close to the derived experimental  $T_e$  value for progression A [ $T_e = 34\,367$  (expt), 35 089 (calc) cm<sup>-1</sup>]. Moreover, the computed vibrational frequency for the 2<sup>1</sup>Π<sub>g</sub> state is small, as we observe for progression A [ $\omega_e = 117$  (expt), 63 (calc) cm<sup>-1</sup>]. The derived vibrational constants for progression A yield a very high extrapolated energy for the dissociation

asymptote. The 2<sup>1</sup>Π<sub>g</sub> state lies above the Ga(4p) + Ga(5s) asymptote<sup>33</sup> and presumably dissociates diabatically to Ga(4p) + Ga(5p). It should be noted that one and two molecular electronic states of <sup>1</sup>Π<sub>g</sub> symmetry emanate from the Ga(4p) + Ga(5s) and Ga(4p) + Ga(5p) asymptotes, respectively. [The 1<sup>1</sup>Π<sub>g</sub> state correlates with the ground Ga(4p) + Ga(4p) asymptote.<sup>32,33</sup>] The above considerations suggest that there is a curve crossing between the 2,3<sup>1</sup>Π<sub>g</sub> states associated with the Ga(4p) + Ga(5s) and Ga(4p) + Ga(5p) asymptotes.

More problematic with the available ab initio information are assignments for the upper electronic states of progressions C and D. We see in Table 5 that there is only one excited electronic state listed whose excitation energy is less than that of the 3<sup>3</sup>Π<sub>g</sub> state and which can be accessed by an electric-dipole transition from the X<sup>3</sup>Π<sub>u</sub> state, namely, the 2<sup>3</sup>Π<sub>g</sub> state. This electronic state has a considerably lower excitation energy and vibrational frequency than those estimated for the upper states of progressions C and D. Moreover, this state is predicted<sup>32</sup> to dissociate to the Ga(4p) + Ga(5s) asymptote.

Alternate assignments for the upper states of progressions C and D would necessarily involve electronic states correlating with either the Ga(4p) + Ga(5p) or, possibly, Ga(4p) + Ga(5s) asymptotes. States correlating with the latter asymptote would have potential energy curves with a significant barrier at large  $R$  to dissociation. There are, in fact, a large number of states which correlate with these asymptotes (12 and 4 states, respectively, of both singlet and triplet multiplicity). While many of these will be repulsive, properties of only a subset of these have been reported in the ab initio calculations.<sup>32,33</sup>

The structured nature of the bands in progressions C and D (see Figure 6) is unexpected. Das<sup>33</sup> has calculated the energies of the fine-structure levels of the X<sup>3</sup>Π<sub>u</sub> electronic state. The lowest of these is the  $\Omega = 0_u^-$  level, and the  $\Omega = 0_u^+$  level is computed to lie 14 cm<sup>-1</sup> higher. The remaining two fine-structure levels ( $\Omega = 1_u$  and  $2_u$ ) lie considerably higher in energy (218 and 467 cm<sup>-1</sup>, respectively). If the spin-orbit relaxation is efficient in the free-jet supersonic expansion, then the dominant fine-structure level populated in the beam will be the ground  $\Omega = 0_u^-$  level. Radiative transitions from this level are allowed to  $\Omega = 0_g^-$  and  $1_g$  excited levels only. It is hard to reconcile these selection rules for individual fine-structure transitions with the complicated band profiles shown in Figure 6. Similar difficulties arise if it is assumed that spin-orbit relaxation is slow, with all fine-structure levels having significant population.

Despite the uncertainties in the assignment of the excited electronic states, the identity of the molecular carrier as Ga<sub>2</sub> is very secure. This identification comes from several pieces of evidence. The isotope splittings and the relative intensities of the assigned isotopomer bands proves that the carrier contains two Ga atoms. The resolvable isotope splittings in progressions A and B preclude the possibility that the molecular carrier contains any light atoms (H or C), since the change in reduced mass upon Ga isotope substitution would be very small and not lead to observable isotope splittings. Moreover, the spectral positions were independent of the composition of the seed gas. Finally, the derived upper bound for the ground-state dissociation energy is consistent with previous experimental and computational estimates of the dissociation energy of Ga<sub>2</sub>. It is hoped that the present study will stimulate further theoretical study of the electronic states of the gallium dimer.

**Acknowledgment.** This research has been supported by the Air Force Office of Scientific Research, under Grant No. F49620-01-1-0183.



## References and Notes

- (1) Morse, M. D. *Chem. Rev.* **1986**, 86, 1049.
- (2) Morse, M. D. In *Metal and Semiconductor Clusters*; Duncan, M. A., Ed.; JAI Press: Greenwich, CT, 1993; p 83.
- (3) Barden, C. J.; Rienstra-Kiracofe, J. C.; Schaefer, H. F. *J. Chem. Phys.* **2000**, 113, 690.
- (4) Langridge-Smith, P. R. R.; Morse, M. D.; Hansen, G. P.; Smalley, R. E.; Merer, A. J. *J. Chem. Phys.* **1984**, 80, 593.
- (5) Zee, R. D. V.; Blankespoor, S. C.; Zwier, T. S. *J. Chem. Phys.* **1988**, 88, 4650.
- (6) Bishea, G. A.; Morse, M. D. *J. Chem. Phys.* **1991**, 95, 5646.
- (7) Simard, B.; Hackett, P. A.; James, A. M.; Langridge-Smith, P. R. *Chem. Phys. Lett.* **1991**, 186, 415.
- (8) Spain, E. M.; Behm, J. M.; Morse, M. D. *J. Chem. Phys.* **1992**, 96, 2511.
- (9) Spain, E. M.; Morse, M. D. *J. Chem. Phys.* **1992**, 97, 4641.
- (10) Ram, R. S.; Jarman, C. N.; Bernath, P. F. *J. Mol. Spectrosc.* **1992**, 156, 468.
- (11) Doverstål, M.; Lindgren, B.; Sassenberg, U.; Arrington, C. A.; Morse, M. D. *J. Chem. Phys.* **1992**, 97, 7087.
- (12) James, A. M.; Powalczyk, P.; Fournier, R.; Simard, B. *J. Chem. Phys.* **1993**, 99, 8504.
- (13) James, A. M.; Kowalczyk, P.; Simard, B.; Pinegar, J. C.; Morse, M. D. *J. Mol. Spectrosc.* **1994**, 168, 248.
- (14) Arrington, C. A.; Blume, T.; Morse, M. D.; Doverstål, M.; Sassenberg, U. *J. Chem. Phys.* **1994**, 98, 1398.
- (15) Pinegar, J. C.; Langenberg, J. D.; Arrington, C. A.; Spain, E. M.; Morse, M. D. *J. Chem. Phys.* **1995**, 102, 666.
- (16) Doverstål, M.; Karlsson, L.; Lindgren, B.; Sassenberg, U. *Chem. Phys. Lett.* **1997**, 270, 273.
- (17) Doverstål, M.; Karlsson, L.; Lingren, B.; Sassenberg, U. *J. Phys. B* **1998**, 31, 795.
- (18) Airola, M. B.; Morse, M. D. *J. Chem. Phys.* **2002**, 116, 1313.
- (19) Hostutler, D. A.; Li, H.; Clouthier, D. J.; Wannous, G. *J. Chem. Phys.* **2002**, 116, 4136.
- (20) Yang, X.; Dagdigian, P. J. *J. Chem. Phys.* **1998**, 109, 8920.
- (21) Tan, X.; Dagdigian, P. J.; Alexander, M. H. *Faraday Discuss.* **2001**, 118, 387.
- (22) Tan, X.; Dagdigian, P. J. *J. Phys. Chem. A* **2001**, 105, 11009.
- (23) Tan, X.; Dagdigian, P. J. *Chem. Phys.* **2002**, 283, 5.
- (24) Ginter, D. S.; Ginter, M. L.; Innes, K. K. *J. Phys. Chem.* **1965**, 69, 2480.
- (25) Douglas, M. A.; Hauge, R. H.; Margrave, J. L. *J. Phys. Chem.* **1983**, 87, 2945.
- (26) Froben, F. W.; Schulze, W.; Kloss, U. *Chem. Phys. Lett.* **1983**, 99, 500.
- (27) Chupka, W. A.; Berkowitz, J.; Giese, C. F.; Inghram, M. G. *J. Phys. Chem.* **1958**, 62, 611.
- (28) Shim, I.; Mandix, K.; Gingerich, K. A. *J. Phys. Chem.* **1991**, 95, 5435.
- (29) Balducci, G.; Gigli, G.; Meloni, G. *J. Chem. Phys.* **1998**, 106, 4384.
- (30) Stowe, A. C.; Kaup, J. G.; Knight, L. B.; Davis, J. R.; McKinley, A. J. *J. Chem. Phys.* **2001**, 115, 4632.
- (31) Cha, C.-Y.; Ganteför, G.; Eberhardt, W. *J. Chem. Phys.* **1994**, 100, 995.
- (32) Balasubramanian, K. *J. Phys. Chem.* **1990**, 94, 7764.
- (33) Das, K. K. *J. Phys. B* **1997**, 30, 803.
- (34) Ghosh, T. K.; Tanaka, K.; Mochizuki, Y. *J. Mol. Struct.* **1998**, 451, 61.
- (35) NIST. *Atomic Spectra Database*, v2.0; National Institute of Standards and Technology: Washington, D. C., 1999.
- (36) Hoffman, B. C.; Sherill, C. D.; Schaefer, H. F. *J. Mol. Struct.* **1996**, 370, 93.
- (37) Allendorf, M. D.; Melius, C. F.; Bauschlicher, C. W. *J. Phys. IV* **1999**, 9 (P8), 23.
- (38) *American Institute of Physics Handbook*; McGraw-Hill: New York, 1972.
- (39) Yang, X.; Dagdigian, P. J. Unpublished work.
- (40) Herzberg, G. *Molecular Spectra and Molecular Structure I. Spectra of Diatomic Molecules*, 2nd ed.; Van Nostrand: Princeton, NJ, 1950.
- (41) Lefebvre-Brion, H.; Field, R. W. *Perturbations in the Spectra of Diatomic Molecules*; Academic: New York, 1986.
- (42) Han, S.; Hettema, H.; Yarkony, D. R. *J. Chem. Phys.* **1995**, 102, 1955.